in vivo *38*: xxx-xxx (2024)
doi:10.21873/invivo.11xxx

No: 7029-K
Please mark the appropriate section for this paper
☒ Experimental
☐ Clinical

Concomitant [18F]F-FAZA and [18F]F-FDG Imaging of Gynecological Cancer Xenografts: Insight Into Tumor Hypoxia

ZITA KEPES[1], EVA HEGEDUS[1], TAMAS SASS[2], CSABA CSIKOS[1,3], JUDIT P. SZABO[1], VIKTORIA SZUGYICZKI[4], ISTVÁN HAJDU[1], ISTVAN KERTESZ[1], GABOR OPPOSITS[1], JOZSEF IMREK[5], LASZLO BALKAY[1], FERENC KRISZTIÁN KALMAN[6] and GYORGY TRENCSENYI[1]

[1]Division of Nuclear Medicine and Translational Imaging, Department of Medical Imaging, Faculty of Medicine, University of Debrecen, Debrecen, Hungary;
[2]Department of Surgery, Faculty of Medicine, University of Debrecen, Debrecen, Hungary;
[3]Gyula Petrányi Doctoral School of Clinical Immunology and Allergology, Faculty of Medicine, University of Debrecen, Debrecen, Hungary;
[4]Department of Nuclear Medicine, Békés County Pándy Kálmán Hospital, Semmelweis, Hungary;
[5]Institute of Physics, University of Debrecen, Debrecen, Hungary;
[6]Department of Physical Chemistry, University of Debrecen, Debrecen, Hungary

Abstract. *Background/Aim: Herein we assessed the feasibility of imaging protocols using both hypoxia-specific [18F]F-FAZA and [18F]F-FDG in bypassing the limitations derived from the non-specific findings of [18F]F-FDG PET imaging of tumor-related hypoxia. Materials and Methods: $CoCl_2$-generated hypoxia was induced in multidrug resistant (Pgp+) or sensitive (Pgp-) human ovarian (Pgp- A2780, Pgp+ A2780AD), and cervix carcinoma (Pgp- KB-3-1, Pgp+ KB-V-1) cell lines to establish corresponding tumor-bearing mouse models. Prior to [18F]F-FDG/[18F]F-FAZA-based MiniPET imaging, in vitro [18F]F-FDG uptake measurements and western blotting were used to verify the presence of hypoxia. Results: Elevated GLUT-1, and hexokinase enzyme-II expression driven by $CoCl_2$-induced activation of hypoxia-inducible factor-1α explains enhanced cellular [18F]F-FDG accumulation. No difference was observed in the [18F]F-FAZA accretion of Pgp+ and Pgp- tumors. Tumor-to-muscle ratios for [18F]F-FAZA measured at 110-120 min postinjection (6.2±0.1) provided the best contrasted images for the delineation of PET-oxic and PET-hypoxic intratumor regions. Although all tumors exhibited heterogenous uptake of both radiopharmaceuticals, greater differences for [18F]F-FAZA between the tracer avid and non-accumulating regions indicate its superiority over [18F]F-FDG. Spatial correlation between [18F]F-FGD and [18F]F-FAZA scans confirms that hypoxia mostly occurs in regions with highly active glucose metabolism. Conclusion: The addition of [18F]F-FAZA PET to [18F]F-FGD imaging may add clinical value in determining hypoxic sub-regions.*

Correspondence to: Dr. Zita Képes, Division of Nuclear Medicine and Translational Imaging, Department of Medical Imaging, Faculty of Medicine, University of Debrecen, Nagyerdei St. 98, H-4032 Debrecen, Hungary. Tel: +36 (70)3646025, e-mail: kepes.zita@med.unideb.hu

Key Words: Cervix xenotransplants, [18F]F-FAZA, [18F]F-FDG, GLUT-1 transporter, hexokinase enzyme-II, hypoxia-inducible factor-1α (HIF-1α), hypoxia, preclinical, positron emission tomography (PET), ovarian xenotransplants.

Hypoxia-inducible factors (HIF) govern the effects of hypoxia on tumor cells and tumor microenvironment (1). Under hypoxic conditions, the dimerization of subunit-α (HIF-1α) and subunit-β (HIF-1β) of HIF-1 is followed by the binding of the active transcription factor (HIF-1) to the hypoxia-responsive elements (HREs), that trigger the expression of a network of genes associated with pro-angiogenic processes and metastatic spread as well as increased resistance to chemo- and radiotherapy (2-5). Besides oxygen depletion, the expression of ABC transporter permeability glycoprotein (P-Glycoprotein, Pgp or ABCB1) further contributes to the development of therapeutic resistance (6). Pgp-stimulated multidrug resistance is considered one of the major causes of treatment failure in gynecological malignancies such as ovarian and cervix cancer (7-9).

Since tumor-related hypoxia results in poor prognosis and inefficient therapeutic outcome (10), the identification of hypoxic tumor regions seems to be a prerequisite prior to definitive oncological treatment.

Positron emission tomography (PET) allows for non-invasive, real-time cancer diagnosis coupled with the opportunity to track anti-tumor therapeutic response (11) and elaborate treatment guidelines (11). Hence the establishment of PET radiopharmaceuticals designed to visualize oxygen deficient intratumor areas has recently come into the focus of research.

Due to the appropriate properties of Fluorine-18 (^{18}F) such as its ideal half-life ($T_{1/2}$: 109.8 min), advantageous decay characteristics (high positron abundance: β≥97%, low β^+ energy: E_{max} and E_{mean}: 0.635 MeV and 0.250 MeV; respectively), short diffusion range (within tissue) and its seamless synthesis in great quantities with high specific activity, it emerged as the most widely used radiolabeling entity of different molecules (12-15). Its half-time not only ensures the coverage of extended exam periods but also limits unintended radiotoxicity that constitutes a clear advantage in *in vivo* applications.

The fact that low-oxygenated cells over-express different transporters (GLUT-1 and GLUT-3) and enzymes (hexokinase enzyme-II/HK-II) (16-18) that are the central regulators of cellular glucose uptake and metabolism in malignant tumors (19, 20), offers a scientifically justifiable rationale for the application of PET imaging with 2-[^{18}F]Fluoro-2-deox y-D-glucose ([^{18}F]F-FDG) to detect hypoxia in different neoplasms. An ample amount of preclinical evidence supports the correlation between [^{18}F]F-FDG accumulation and oxygen deprived cells or hypoxic tumor regions (21-24). For example, hypoxia-induced (<0.002% O_2) [^{3}H]H-FDG uptake elevation by MCF7 human breast carcinoma cells was reported by Burgman *et al*. *in vitro* (18). Despite the promising results, however, increased [^{18}F]F-FDG uptake associated with infectious or inflammatory processes (25) may bring obstacles in distinguishing malignant tracer accumulation from infection/inflammation-associated radiopharmaceutical uptake.

[^{18}F]F-fluoroazomycin arabinoside ([^{18}F]F-FAZA), a member of 2-nitroimidazole compound family, is a viable alternative to [^{18}F]F-FDG for the PET imaging of hypoxia (26). Followed by passive diffusion *via* the cell membrane, [^{18}F]F-FAZA is reduced and its reactive metabolites interact with cellular components under hypoxia leading to the metabolic trapping of the radiotracer and the selective demarcation of less-oxygenated regions (27, 28). Compared to its first generation predecessor, [^{18}F]F-fluoromisonidazole ([^{18}F]F-FMISO), the lower lipophilicity of [^{18}F]F-FAZA ensures increased accumulation along with rapid wash-out from off-target tissues/organs that results in superior pharmacokinetics and hypoxia/normoxia contrast (26, 29, 30). Encouraging results obtained from experiments small animal models of MDA-MB231 and MCF-7 breast cancers (31), SiHa cervix carcinoma (32), A431 squamous cell carcinoma (33) and esophageal adenocarcinoma (EAC) (34) have confirmed the feasibility of [^{18}F]F-FAZA as a hypoxia-specific radiopharmaceutical for PET imaging purposes (35).

Based on these findings we hypothesize that the application of imaging protocols using both [^{18}F]F-FAZA and [^{18}F]F-FDG for hypoxia assessment may aid to counteract the non-specificity of single [^{18}F]F-FDG PET imaging. Therefore, our intention was to compare the [^{18}F]F-FAZA and [^{18}F]F-FDG uptake patterns of female CB17 severe combined immunodeficient (SCID) mice bearing multidrug resistant (Pgp-) or multidrug sensitive (Pgp+) human ovarian, and cervix carcinoma xenografts (ovarian: A2780 Pgp- and A2780AD Pgp+; cervix: KB-3-1 Pgp-, KB-V-1 Pgp+). Prior to *in vivo* imaging, the capability of [^{18}F]F-FDG to detect chemically-induced (with cobalt dichloride/$CoCl_2$) hypoxia *in vitro* was tested, and we determined the effect of oxygen deprivation on the cellular expression of GLUT-1 protein and HK-II enzyme.

Materials and Methods

Radiochemistry, metabolic stability and logp. Both [^{18}F]F-FDG and [^{18}F]F-FAZA were produced in the radiochemistry laboratory of the Division of Nuclear Medicine and Translational Imaging, Department of Medical Imaging, Faculty of Medicine, University of Debrecen (Debrecen, Hungary) according to the methods of Hamacher *et al*. and Reischl *et al*. (36, 37). The sterile products were used for PET imaging after quality control.

Briefly, 5 mg of precursor 1-(2,3-diacetyl-5-tosyl-α-d-arabinofuranosyl)-2-nitroimidazole in 1 ml of dimethyl sulfoxide was reacted with the following mixture at 100˚C for 5 min: azeotropically dried [^{18}F]F-fluoride, 15 mg of Kryptofix 2.2.2. (Merck, Darmstadt, Germany), and 3.5 mg of K_2CO_3. Then, the reaction cocktail was subjected to a two-min-long hydrolysis using 1 ml of 0.1N NaOH at 30˚C and cooled down to 40˚C. Thereafter, the crude mixture was passed through a series of Macherev-Nagel (Symetron Ltd., Budapest, Hungary) SPE columns composed of a cation exchanger (PS-H+, large), an anion exchanger (2 pieces of Chromafix PS-OH-, large), a neutral alumina (Alox N, large), and a reverse phase (2 pieces of HR-P, large). Prior to usage, the columns were preconditioned first with 20 ml of ethanol, and then with 100 ml of sterile and bacterial endotoxin-free water. Afterwards, 2 ml of 80% ethanol was applied to rinse the reaction vessel, and to wash the column. Finally, [^{18}F]F-FAZA was recovered with 12 ml of 15% ethanol, collected in vial composed of 1.7 ml of 10% NaCl and 0.7 ml of 1M NaH_2PO_4.

The radiochemical purity (RCP) was assessed with the use of an HPLC system with Supelco Discovery® Bio Wide Pore C-18 column (250 mm×4.6 mm; particle size: 10 μm) coupled with a radiodetector. Signals were simultaneously detected with both a radio and an absorbance detector at 254 nm.

The *logp* value of [^{18}F]F-FAZA was assessed by the serial determination of the retention time of FAZA on a RP HPLC column (Waters Resolve C18 Radial-Pak Column, 90Å; Waters Corporation,

Milford, MA, USA) that was followed by the comparison of the measured *logp* value with the one known from the reference literature (26). Since our results were in good correlation with those of the reference data, the given *logp* value was accepted. [^{18}F]F-FDG is a routinely produced radiotracer for the PET examinations of oncological patients.

Cell culturing, $CoCl_2$ treatment. Drug sensitive (Pgp+) and non-sensitive (Pgp-) human ovarian (Pgp- A2780 and Pgp+ A2780AD) and epidermoid cervix carcinoma (Pgp- KB-3-1 and Pgp+ KB-V-1) cell lines were used. The cells were cultured under standard laboratory circumstances in Dulbecco's Modified Eagle Medium (DMEM, Merck) supplemented with 10% foetal bovine serum (FBS, Thermo Fisher Scientific Inc., Waltham, MA, USA) in incubators with 5% CO_2 and 95% humidity at 37˚C. The viability of the cells was verified using trypan blue exclusion test. The passage of the cells was performed every three days. The Pgp+ cell lines were grown in the presence of their corresponding chemotherapeutic agents; 28 μM Doxorubicin and 20 μM Vinblastin were used for the cultivation of A2780AD and KB-V-1 cells, respectively. The drugs were withdrawn from both Pgp+ cell lines during the passage before radiopharmaceutical injection. To induce chemical hypoxia the cells were treated with 250 μM $CoCl_2$ for 24 or 48 h. According to literature data, $CoCl_2$ is commonly used to artificially generate hypoxia, as it is able to inhibit the degradation of HIF-1α by blocking the activity of HIF-1α-prolyl hydroxylases (38, 39).

Experimental animals, animal housing. Twelve-week-old female CB17 SCID mice (n=10) ranged in weight from 18 to 22 g were purchased from Innovo Ltd. (Isaszeg, Hungary). All mice were bred in pathogen-free IVC cages (Techniplast, Akronom Ltd., Budapest, Hungary) in a temperature (26±2˚C) and humidity (50±5%) controlled room with a 12-h light/12-h dark schedule (Division of Nuclear Medicine and Translational Imaging, Faculty of Medicine, University of Debrecen, Debrecen, Hungary). Free access to sterile semi-synthetic rodent chow (Charles River Ltd., Gödöllő, Hungary) and sterilized water was ensured for all experimental animals. The Ethics Committee for Animal Experimentation of the University of Debrecen approved this study (study number: 8/2016/DEMÁB). The experiments were carried out according to the regulations of the Animal Experimentation Committee of the UK (40).

Tumor induction. Subcutaneous tumor models were generated by the implantation of Pgp- A2780/KB-3-1 cells (3×10^6/150 μl physiological saline) and their corresponding Pgp+ counterparts (5×10^6/150 μl physiological saline) in the left and right thigh of the study mice, respectively. Tumor induction was performed under isoflurane-induced anaesthesia using 3% and 1.5% Forane (AbbVie, Budapest, Hungary) for induction and maintenance, respectively, with 0.4 l/min O_2 (Linde Healthcare, Budapest, Hungary), and 1.2 l/min N_2O (Linde Healthcare); and throughout the whole process sterile conditions were maintained. To assess the organ distribution of the investigated radiotracers, 20±1 days post tumor cell inoculation all mice were subjected to *in vivo* uptake studies at an average tumor volume of 39.12±3.34 mm^3.

Western blotting. To identify HIF-1α, GLUT-1, and HK-II expression, western Blot analyses were performed using whole cell lysates. For the analyses sodium dodecyl sulfate-polyacrylamide gel electrophoresis (SDS-PAGE) was applied, during which 100 μl of electrophoresis buffer with a fivefold concentration was added to the samples and boiled for 10 min. Sixty μg of protein were separated on a 7.5% SDS-PAGE gel. The protein content of the gel was transferred to a nitrocellulose membrane. PBST with 5% non-fat dry milk powder was used to inhibit non-specific protein interactions between the cell membrane and the antibodies. After blocking, the membranes were washed and incubated overnight with the primary antibodies at 4˚C. The primary antibodies were diluted according to the manufacturer's recommendation (Abcam Inc., Cambridge, MA, USA). Following a 30-min long wash with PBST, the membranes were incubated with the secondary antibodies (anti-rabbit IgG; Bio-Rad Laboratories, Hercules, CA, USA) for an hour at room temperature. The secondary antibodies were used at a dilution of 1:1,000 in PBS containing 1% non-fat dry milk powder. Signals were visualized using chemiluminescence based on the manufacturer's instructions (Pierce, Rockford, IL, USA).

In vitro [^{18}F]F-FDG uptake studies. The control and the $CoCl_2$-treated cells (1×10^6/ml) were preincubated with 5 mM D-glucose containing PBS for 10 min at 36˚C, that was followed by the addition of 0.37 MBq/ml of [^{18}F]F-FDG to both samples. Incubation with [^{18}F]F-FDG was further proceeded for the indicated time in each experiment. Cold PBS was added to stop cellular [^{18}F]F-FDG tracer uptake, then the cells were washed three times with the same solution and radioactivity was measured in a calibrated gamma counter at the [^{18}F]F energy level (Canberra-Packard Gamma counter type Cobra II, Canberra Packard Central Europe GmbH, Schwadorf, Austria). The results were decay corrected and the radiopharmaceutical uptake was presented as counts per minute^{-1} (10^6 cells)$^{-1}$ [cpm]. The cellular tracer accumulation was also listed as a percentage of the incubating activity (ID%), that indicates what percentage of the [^{18}F]F-FDG activity in the external solution is taken up by 1 million cells. The fact that [^{18}F]F-FAZA is able to attach to intracellular macromolecules only under hypoxic conditions, and $CoCl_2$-induced hypoxia was developed in a normoxic environment explains why we carried out *in vitro* uptake studies only with [^{18}F]F-FDG.

PET scans, image data analyses. [^{18}F]F-FDG and [^{18}F]F-FAZA PET examinations were performed to determine tumor hypoxia. PET imaging was conducted on the MiniPET-II (DE-ATOMKI, Debrecen, Hungary) device of the Division of Nuclear Medicine and Translational Imaging, Department of Medical Imaging, Faculty of Medicine, University of Debrecen. The MiniPET-II scanner contains 12 detector modules, 12×35×35 LYSO scintillator crystal blocks and position sensitive PMTs. Its resolution is 1.1 mm, the field of view (FOV) is 5 cm, and the sensitivity of the system is 11.4%.

Approximately 7 MBq of [^{18}F]F-FDG or [^{18}F]F-FAZA in a final volume of 200 μl of saline were injected into the study animals *via* the lateral tail vein. During the 20-min static [^{18}F]F-FDG PET acquisition, which started 40 min after radiopharmaceutical injection, isoflurane-induced anesthesia was maintained (1.5% Forane, 0.4 l/min O_2, and 1.2 l/min N_2O). In case of [^{18}F]F-FAZA PET imaging, both static and dynamic scans were obtained also under inhalation anesthesia. During static imaging, data were gathered for 20 min from the 120th min post tracer injection.

For the quantitative assessment of radiotracer uptake, standardized uptake values (SUV) were registered from 3-

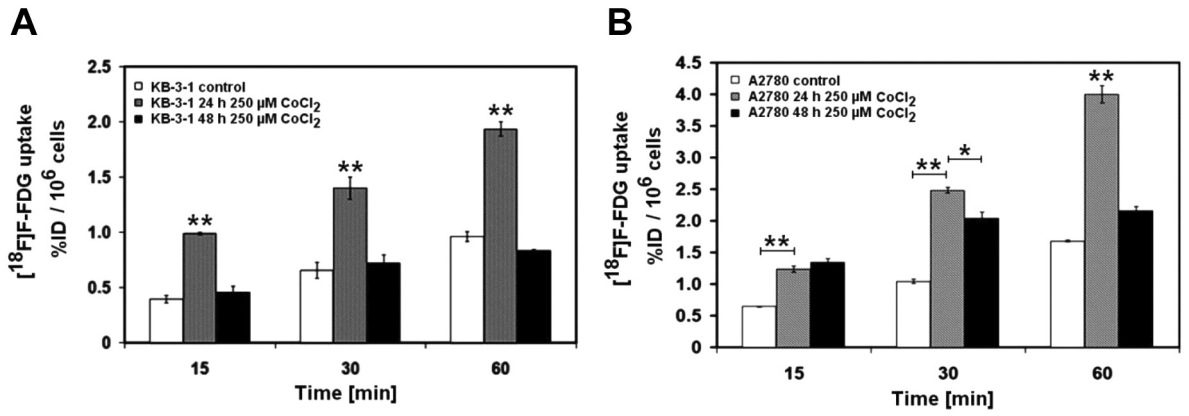

Figure 1. *[18F]F-FDG uptake by KB-3-1 and A2780 cells. [18F]-Fluorodeoxyglucose; [18F]: Fluorine-18 ([18F]F-FDG) accumulation in KB-3-1 cells incubated with $CoCl_2$ for 24 and 48 hs, and the radioactivity in control KB-3-1 cells (Panel A). The [18F]F-FDG uptake by KB-3-1 cells incubated for 24 h was significantly higher at all investigated time points compared both to the untreated control cells and to cells that were incubated for 48 h. The [18F]F-FDG uptake by A2780 cells administered with $CoCl_2$ for 24 and 48 h and the radioactivity in the control A2780 cells (Panel B). The radioactivity in A2780 cells treated for 24 h was remarkably higher at the 30- and 60-min time points in comparison with the naïve control cells as well as cells administered with $CoCl_2$ for 48 h. At the 15 min time point, the [18F]F-FDG accretion in the A2780 cells incubated for 24 h was considerably higher than the radioactivity in the untreated cells. *p≤0.05; **p≤0.01.*

dimensional ellipsoidal volume of interests (VOIs) manually placed over selected tissues and organs with BrainCad image analysis software. SUV was expressed in terms of maximum (SUV_{max}) indicating the voxel with the highest radioactivity, and average (SUV_{mean}) that reflects the average activity of all voxels in the region concerned. SUV calculation was conducted using the following formula:

SUV=[VOI activity (Bq/ml)]/
[injected activity (Bq)/animal weight (g)].

Upon quantitative assessment tumor-to-background/muscle (T/M) ratios were also estimated to directly compare the tracer accumulation of the organs/tissues and that of the background.

Statistical analyses. Statistical differences were calculated by unpaired two-tailed *t*-tests, one-way ANOVA, or two-way ANOVA. Data are displayed as mean±SD of at least three independent experiments, and changes with $p<0.05$ were regarded significant, unless otherwise indicated.

Results

Radiochemistry. [18F]F-FAZA was produced with high specific activity, and it was free of any non-radioactive impurity. The RCP generally exceeded 95%. The decay corrected radiochemical yield (RCY) was shown to be 20-25% in 50 min. The estimated *logp* value for [18F]F-FAZA was 1.1, that indicates the lipophilic character of the imaging probe. The results of urine TLC analyses showed that unchanged [18F]F-FAZA accounted for approximately 90% and 73% of the detected radioactivity 10 and 60 min post tracer injection; respectively.

Based on the obtained radiochemical data, [18F]F-FAZA was suitable for the performance of further *in vivo* examinations.

In vitro investigations. Nuclear medicine ([18F]F-FDG) and molecular biological methods (western blot and immunocytochemistry) were used to assess hypoxia and related processes in KB-3-1 and A2780 cells treated with 250 µM $CoCl_2$ for 24 or 48 h. Based on the results obtained, $CoCl_2$ treatment induced the over-expression of GLUT-1 glucose transporter and HK-II.

Assessment of KB-3-1 cells. Cellular [18F]F-FDG uptake. As presented in Figure 1, Panel A, uptake of [18F]F-FDG was gradually increased over time until 60 min in all cell groups with the highest uptake values being detected in case of the cells administered with $CoCl_2$ for 24 h. Further assessing the [18F]F-FDG accumulation in KB-3-1 cells, significantly higher radioactivity was observed in cells treated with $CoCl_2$ for a day at the 15, 30, and 60 min time points compared to the tracer uptake in the control cells and KB-3-1 cells that were incubated with $CoCl_2$ for 48 h (Figure 1, Panel A).

Western blot. The levels of HIF1-α, GLUT-1 and HK-II were examined using western blot. Depending upon the length of incubation with $CoCl_2$, varying degrees of protein over-expression were obtained. Regardless of treatment duration, $CoCl_2$ induced the expression of all investigated proteins compared to the control that supports the higher [18F]F-FDG uptake of the treated cells in comparison with their treatment-naïve counterparts. As seen in Figure 2, Panel A

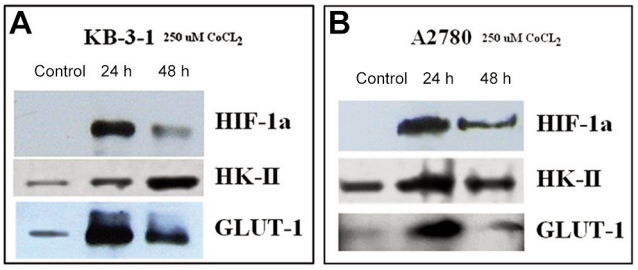

Figure 2. *Western blot analyses of $CoCl_2$-treated KB-3-1 and A2780 cells and their control counterparts. Expression levels of HIF-1α, HK-II enzyme, and GLUT-1 transporter in $CoCl_2$-incubated KB-3-1 (Panel A), and A2780 (Panel B) cells as well as in control KB-3-1 (Panel A) and A2780 (Panel B) cells.*

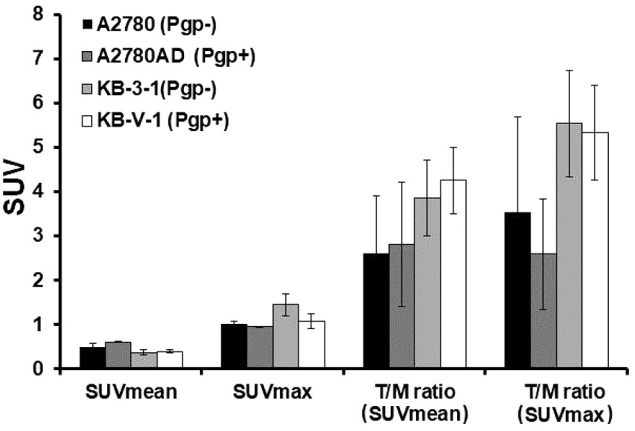

Figure 3. *Quantitative assessment of the [18F]F-fluoroazomycin arabinoside ([18F]F-FAZA) uptake by the investigated Pgp+ and Pgp- tumor xenografts. The standardized uptake value (SUV) (mean and max) values and the tumor-to-muscle (T/M) ratios (mean and max) of permeability glycoprotein (Pgp)- A2780 and KB-3-1 and Pgp+ A2780AD and KB-V-1 tumor xenografts for [18F]F-FAZA are demonstrated.*

there was a meaningful increment in the levels of HIF1-α and GLUT-1 transporter following a 24-h long treatment compared both to the control and the 48-h long treatment. The highest HK-II enzyme expression was detected upon the 48-h long incubation (displayed in Figure 2, Panel A).

In vitro assessment of A2780 cells. Cellular [18F]F-FDG uptake. Analysing the [18F]F-FDG uptake of the A2780 cells, we found that the radiotracer accumulation in the treated cells increased compared to the control cells at all investigated time points. Nevertheless, notable differences were found between the different treatment regimes. As shown in Figure 1, Panel B, no considerable difference was found between the radioactivity of the cells treated with $CoCl_2$ for 24 and 48 h at the first examination point post tracer administration (15 min). After 30 min of [18F]F-FDG injection, there was a non-significant difference in tracer uptake between treated and control cells. The difference became statistically significantly only at 60 min, and A2780 cells that were incubated with $CoCl_2$ for 24 h presented higher [18F]F-FDG concentration than those incubated for 48 h. Figure 1, Panel B demonstrates the radiopharmaceutical uptake values of the A2780 cells.

Western blot. The results of the western Blot analyses revealed that the expression of hypoxia-related HIF1-α notably increased in the $CoCl_2$-administered cells relative to the untreated ones, in particular in cells incubated for 24 h (Figure 2, Panel B). In addition, the levels of GLUT-1 transporter that transports [18F]F-FDG and the amount of HK-II enzyme that is responsible for its phosphorylation were also higher in cells subjected to the 24-h long treatment.

In vivo MiniPET examinations. Static and dynamic MiniPET examinations were performed on the hypoxic tumors of CB17 SCID female mice applying the MiniPET-II small animal device of the Division of Nuclear Medicine and Translational Imaging, Department of Medical Imaging, Faculty of Medicine, University of Debrecen.

Static MiniPET examinations with [18F]F-FAZA. Approximately 20 days post tumor cell inoculation (20±5 days) and at an average tumor volume of 400±80 mm^3, [18F]F-FAZA PET imaging was conducted on the experimental animals. Based on existing guidelines, 20-min static scans were obtained on the tumors 120 min post [18F]F-FAZA injection. According to the results of the quantitative PET data analyses, no significant difference was found between the SUV_{mean} values of the tumors with respective values being 0.48±0.095, 0.60±0.015, 0.37±0.05 and 0.39±0.03 for the Pgp- A2780, Pgp+ A2780AD, Pgp- KB-3-1, and Pgp+ KB-V-1 tumors, respectively. Regarding the mean T/M ratios, two-to-four fold higher [18F]F-FAZA accumulation was observed in all tumors compared to the background (muscle), however, the differences between them were not statistically significant (mean T/M ratios for Pgp- A2780, Pgp+ A2780AD, Pgp- KB-3-1, and Pgp+ KB-V-1 tumors: 2.6±1.29, 2.8±1.4, 3.85±0.84, and 4.25±0.75; respectively). The results of the quantitative PET image evaluation are given in Figure 3.

Dynamic MiniPET examinations with [18F]F-FAZA. To explore the temporal kinetics of the radiopharmaceutical uptake by the tumors and the background muscle, dynamic PET acquisition was also conducted on the tumors of the xenotransplanted mice injected with [18F]F-FAZA. As displayed in Figure 4, the SUV_{mean} values of the hypoxic tumor regions showed an exponential increase until the 120

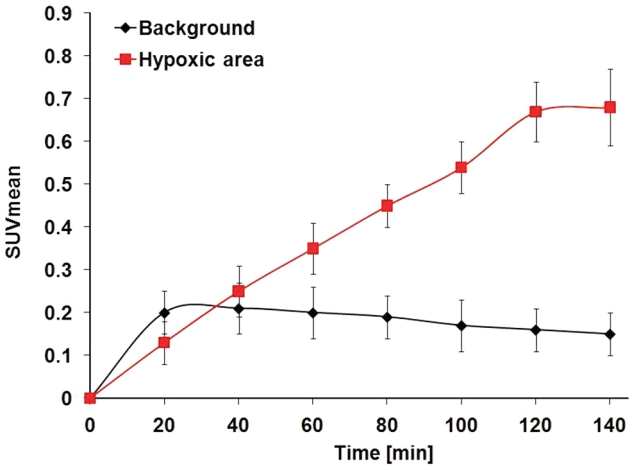

Figure 4. *Temporal kinetics of Fluorine-18 F-fluoroazomycin arabinoside ([18F]F-FAZA) accumulation. The real-time temporal accumulation kinetics of the hypoxic tumor regions and the background (muscle) for [18F]F-FAZA are shown. SUV: Standardized uptake value.*

min time point, that was followed by an equilibrium. On the contrary, however, the accumulation in the muscle showed an increase only until the 30th min, then - due to the absence of hypoxia - [18F]F-FAZA escaped from the muscle cells resulting in the decrease of the tracer concentration (seen in Figure 4). Moreover, the ratio of the radiotracer uptake in the hypoxic tumor area and the background muscle (T/M) appeared to be the highest 110-120 min post radiotracer application (6.2±0.1).

Thee temporal kinetics of the [18F]F-FAZA uptake in the hypoxic and non-hypoxic tumor regions were also evaluated. Panel A and C of Figure 5 display the [18F]F-FAZA accumulation in a representative tumor xenograft (KB-3-1) at 20 min intervals from the radiotracer injection until the 140 min end point. As seen in Figure 5, the SUV_{mean} values of the hypoxic regions exhibited an exponential increase over time, then 120 min after [18F]F-FAZA administration an equilibrium was reached (SUV_{mean}: 0.67±0.07). Similarly, the radioactivity of the non-hypoxic neoplastic territories also presented a slight elevation until the 30 min time point (SUV_{mean}: 0.15±0.05), that was followed by the slow wash-out of the radiopharmaceutical (SUV_{mean}: 0.11±0.05 at the 120 min time point) resulting in the reduction of [18F]F-FAZA accumulation.

MiniPET examinations with [18F]F-FDG and [18F]F-FAZA. The tumor-carrying mice that were examined with hypoxia sensitive [18F]F-FAZA, were also subjected to [18F]F-FDG PET acquisition. The two PET modalities were performed within one day. Figure 6 illustrates representative [18F]F-FDG and [18F]F-FAZA PET images from the xenotransplated small animals. The 20-min static scans acquired 40 min postinjection of [18F]F-FDG on the tumor regions were used for the verification of the viability of the tumors and for the assessment of the intensity of their glucose metabolism. In addition, we searched for intratumor areas with intensive [18F]F-FDG accumulation that were also positive for [18F]F-FAZA.

The distribution of [18F]F-FDG was highly heterogenous in all examined tumor xenografts, indicating that certain intratumor areas have high glucose metabolism. Remarkable differences were observed regarding the SUV_{mean} values of the highly [18F]F-FDG avid tumor regions (SUV_{mean}: 2.72±0.23) and those that did not take up the radioactive glucose analogue (SUV_{mean}: 1.2±0.36). Even greater differences were observed in the case of [18F]F-FAZA, where the radioactivity of the strongly [18F]F-FAZA positive regions (SUVmean: 0.86±0.06) was 6-7 times higher compared to that of the [18F]F-FAZA negative ones (SUVmean: 0.11±0.05) (Figure 7). As presented in Figure 8, the highly [18F]F-FDG positive intratumor areas overlapped with the hypoxic territories accumulating radiotracer [18F]F-FAZA.

Discussion

Chemically-induced hypoxic tumor models underwent [18F]F-FDG and subsequent [18F]F-FAZA PET imaging to test the diagnostic value of dual imaging of tumor-related hypoxia and bypassing [18F]F-FDG-related non-specific accumulation.

In vitro assessment of KB-3-1 and A2780 cells. To verify the presence of hypoxia, western blotting and [18F]F-FDG uptake measurements were accomplished *in vitro*.

Western blot analyses. Based on the results of the western blot analyses, indicating elevated levels of HIF-1α, GLUT-1 transporter and HK-II enzyme in the $CoCl_2$-treated KB-3-1 and A2780 cells, we managed to successfully induce artificially hypoxia in both cell lines, that was consistent with the findings of other research groups (41-43). Vengellur *et al.,* Busch *et al.,* and Guo *et al.,* also used $CoCl_2$ for hypoxia generation in different cells like mouse embryonic fibroblasts (42), human keratinocytes (43) or in leukemic cells (41), and they also verified the over-expression of HIF-1α upon $CoCl_2$ administration.

Inhibiting the activity of prolyl hydroxylase, hypoxia-mimetic $CoCl_2$ stabilizes HIF-1α, that leads to the up-regulated transcription of several proteins such as GLUT-1 transporter and HK-II enzyme (42, 44, 45). Although, accordingly, both incubated cell lines over-expressed GLUT-1 and HK-II compared to the control cells independently of the length of $CoCl_2$ treatment, the observed differences in the degree of the protein expression of the cells incubated

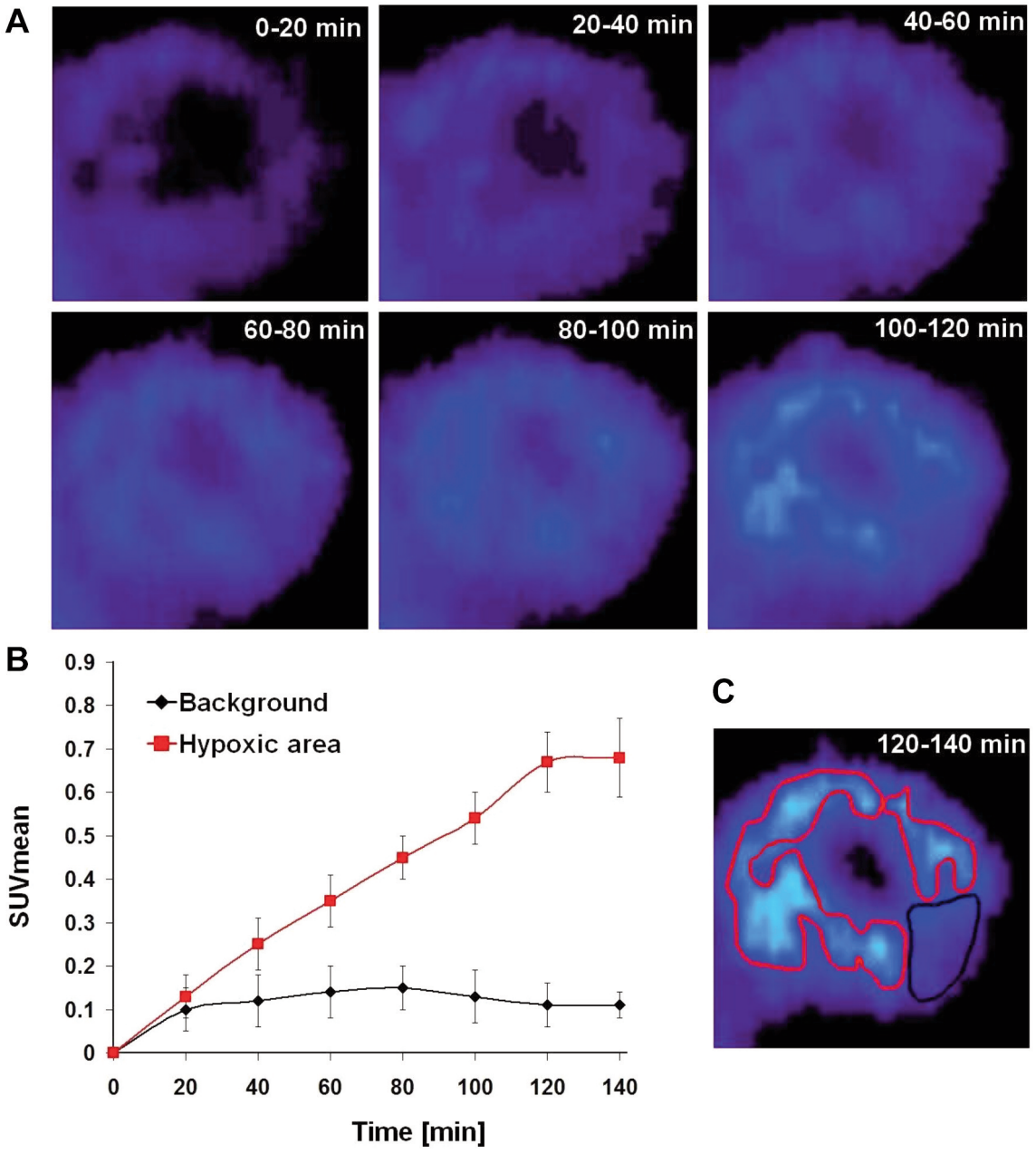

Figure 5. *Temporal kinetics of the Fluorine-18 fluoroazomycin arabinoside ([18F]F-FAZA) accumulation in the hypoxic and non-hypoxic regions of the investigated tumors. [18F]F-FAZA accumulation in a representative tumor xenograft (KB-3-1) at 20 min intervals from the start of the radiotracer injection (0 min) until the end point (140 min) of the dynamic acquisition (Panel A and C). Temporal uptake kinetics of [18F]F-FAZA in the hypoxic (red line) and non-hypoxic (black line) regions of the investigated tumors (Panel B). SUV: Standardized uptake value.*

for different times (24 or 48 h) may imply that the transcription of these molecules could be determined by other factors beyond the presence of hypoxia. In addition, we presuppose that lower GLUT-1 and higher HK-II levels in KB-3-1 cells treated for 48 h compared to those incubated for 24 h may indicate that in case of KB-3-1 cells the uptake of the majority of glucose took place within 24 h requiring enhanced GLUT-1 expression, while its HK-II-based metabolism mostly occurred after 24 h (Figure 2, Panel A). In contrast, immunohistochemistry for both proteins showed the highest membrane expression of GLUT-1 and HK-II in A2780 cells after 24 h treatment, indicating that the cell type may also impact transcription. Similarly to the current findings, ovarian cells subjected to hypoxia (1.5% O_2) also

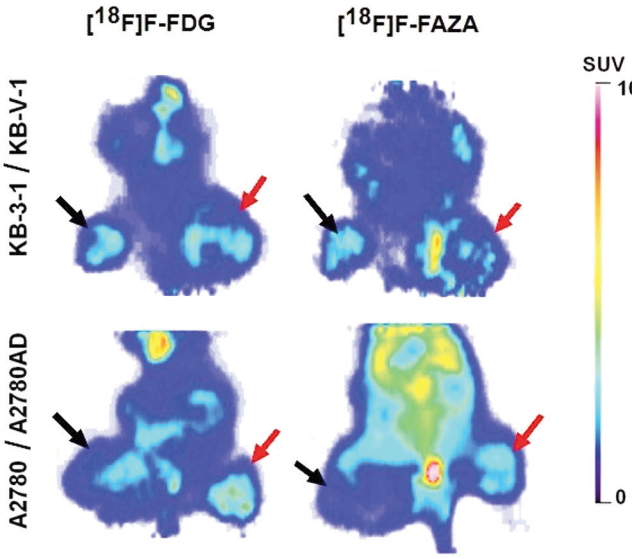

Figure 6. *[18F]F-FDG and [18F]F-FAZA MiniPET examinations of SCID mice xenotransplanted with A2780, A2780AD, KB-3-1, and KB-V-1 tumor cell lines. Representative coronal [18F]F-FDG and [18F]F-FAZA positron emission tomography images of severe combined immunodeficient mice xenotransplanted with A2780, A2780AD, KB-3-1, and KB-V-1 tumor cell lines. Black arrows: Pgp negative tumors; red arrows: Pgp positive tumors. [18F]: Fluorine-18; [18F]F-FDG: [18F]Fluoro-2-deoxy-D-glucose; [18F]F-FAZA: [18F]F-fluoroazomycin arabinoside; SUV: standardized uptake value.*

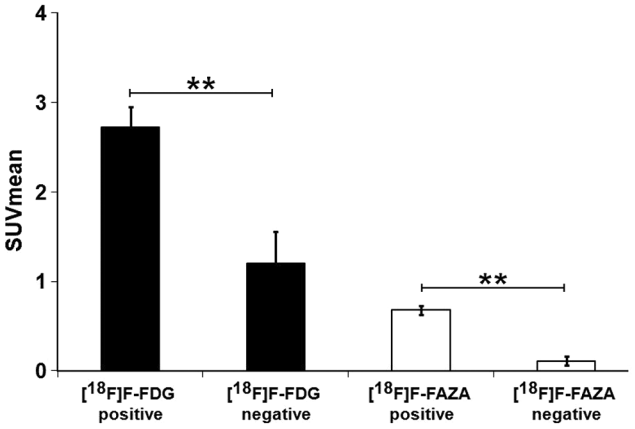

Figure 7. *Quantitative evaluation of intratumor [18F]F-FDG and [18F]F-FAZA radiotracer uptake. Average SUV_{mean} values of the intratumor areas with (+) or without (-) [18F]F-FDG/[18F]F-FAZA accumulation. **p≤0.01. [18F]: Fluorine-18; [18F]F-FDG: [18F]Fluoro-2-deoxy-D-glucose; [18F]F-FAZA: [18F]F-fluoroazomycin arabinoside; SUV: standardized uptake value.*

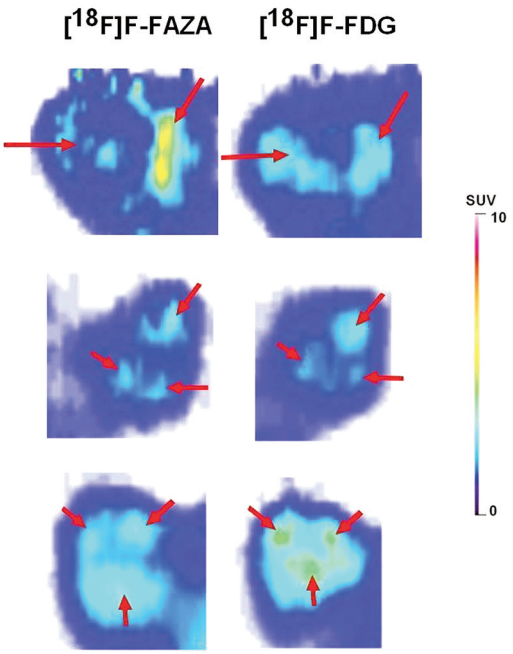

Figure 8. *Representative [18F]F-FDG and [18F]F-FAZA PET images of the hypoxic tumor regions. [18F]F-FDG and [18F]F-FAZA uptake patterns in the hypoxic tumor regions. The red arrows indicate the overlaps between the uptakes of the two radiopharmaceuticals. [18F]: Fluorine-18; [18F]F-FDG: [18F]Fluoro-2-deoxy-D-glucose; [18F]F-FAZA: [18F]F-fluoroazomycin arabinoside; PET: positron emission tomography; SUV: standardized uptake value.*

showed more pronounced GLUT-1 expression than those under atmospheric oxygen (20% O_2) (21). However, no signs of hypoxia associated GLUT-1/HK up-regulation was observed by Burgman *and al.* in MCF-7 breast cancer cells (18), that could also support the role of several factors in the expression of these proteins.

Cellular [18F]F-FDG uptake. Given that both $CoCl_2$-treated hypoxic cell lines demonstrated higher *in vitro* radiopharmaceutical accumulation in association with the presence of HIF-1α, [18F]F-FDG uptake measurements could be successfully used to monitor the presence of chemically-induced hypoxia.

Regarding KB-3-1 cells, the results of the western blot analyses were in accordance with those of the *in vitro* uptake studies. The highest HIF-1α and GLUT-1 expression observed one day after $CoCl_2$ incubation corresponded to the highest [18F]F-FDG uptake measured at 24 h, that strengthened the positive correlation of the radiotracer accretion with low oxygen tension. The analogous immunological outcomes and radioactivity measurements in the case of the A2780 cell line further confirmed the strong association between [18F]F-FDG accumulation and hypoxia. Moreover, consistent with our findings, low oxygenated microenvironment also resulted in elevated [18F]F-FDG/[3H]H-FDG concentration in head and neck squamous-cell carcinoma (UT-SCC-5 and UT-SCC-20) (46), or in androgen-independent (PC-3) and androgen-sensitive

(LNCaP) prostate cancer cell lines (47). Similarly, human small cell lung cancer (SCLC) cell line CPH B54 manifested increased [18F]F-FDG concentration in accordance with up-regulated GLUT-1 transporter (48). Moreover, applying different oxygen atmospheres (0% to 20% O_2), Clavo *et al*. showed a higher increase in [18F]F-FDG uptake in HTB 77 IP3 ovarian and HTB 63 melanoma cells under anoxia/hypoxia (0%, 1.5%, 5% O_2) compared to normoxic circumstances (20% O_2) (21).

Overall, with these [18F]F-FDG uptake measurements, we verified the presence of hypoxia in both cell lines.

In vivo MiniPET examinations. Static [18F]F-FAZA PET imaging. The heterogenous radiopharmaceutical accumulation detected upon the analyses of the [18F]F-FAZA PET images indicated nonhomogenously distributed hypoxic areas within the tumors, that could be largely attributed to the dynamic character of hypoxia, hypoxia-related alterations in the tumor microenvironment, adaptive metabolic changes, or changes associated with tumor progression. Consistent with our findings, HCT116 colorectal tumor xenografts were similarly characterized by uneven [18F]F-FAZA uptake (49). Likewise, advanced stage non-small cell lung cancers (NSCLC) and head and neck tumors also exhibited heterogenous hypoxia maps in previous clinical studies applying [18F]F-FAZA or the first generation nitroimidazole compound [18F]F- FMISO (50-52).

Since the SUV_{mean} values of drug resistant and drug sensitive tumors did not differ significantly, we assume that the presence of Pgp had no considerable impact on radiotracer uptake during the course of the experiment. However, prolonged examination periods and related longer incubations with chemotherapeutic drugs are required to strengthen our hypothesis.

High-contrasted [18F]F-FAZA images provided by the two-to-four times higher radiotracer accretion of the tumors compared to the background muscle ensured the precise delineation of the oxygen deficient tumor subregions from the surrounding tissues/organs with abundant oxygenation (T/M ratios were 2.6±1.29, 2.8±1.4, 3.85±0.84 and 4.25±0.75 for the A2780, A2780AD, KB-3-1 and KB-V-1 tumors, respectively). The experienced improved image quality could be assigned to the favorable solubility of [18F]F-FAZA, that allows for higher uptake and prompt blood clearance, thereby providing better signal-to-noise ratios even at early investigation time points. Prior preclinical results on tumor-to-background ratios determined in experimental models of EAC and SCCVII squamous carcinoma are consistent our findings (34, 53). Moreover, recent data established that the T/M ratios of [18F]F-FAZA appear to overpass those of other nitroimidazole derivatives like [18F]flortanidazole (HX4) or [18F]F-FMISO (54-56).

Dynamic [18F]F-FAZA PET imaging. To monitor the real time *in vivo* tracer kinetics, dynamic [18F]F-FAZA PET acquisition was performed. Consistent with earlier preclinical findings (56) the maximum T/M ratio for [18F]F-FAZA was recorded at 120 min post tracer administration (6.2±0.1). Comparing hypoxia PET tracers in WAG/Rij rats bearing rhabdomyosarcoma R1, Peeters *et al*. also observed the highest T/M ratio 2 h after [18F]F-FAZA injection (4.0±0.5) (56). Identically, [18F]F-FAZA showed the greatest tumor-to-off-target contrast values at the same time point in studies with head and neck and lung cancers, that also corroborated with our observations (30, 57, 58). Based on these results, it seems that the PET-oxic and hypoxic regions could be best differentiated 2 h postinjection of [18F]F-FAZA, making it the optimal time for image acquisition.

Similarly to our records, [18F]F-FAZA demonstrated plateau in the tumors at around 120 min in dogs with spontaneous malignancies (59) and in small animal hypoxic tumor models (56). Given that in the absence of hypoxia the reactive form of [18F]F-FAZA is reoxidized, that is followed by the efflux of the radiopharmaceutical from the cells (27), the highest tracer uptake was reached earlier (30 min) in well oxygenised regions (muscle). In contrast, Choen *et al*. registered the maximal muscle concentration for [18F]F-FAZA at a later time point (60 min post tracer application) (59).

[18F]F-FDG PET imaging. Since hypoxia-associated HIF-1α mediates the expression of GLUT transporters that are the major determinants of [18F]F-FDG uptake (50, 60), the results of [18F]F-FDG PET indicating heterogenous tracer distribution confirm non-homogenous hypoxia pattern within the assessed gynecological tumors. In addition, the notable differences between the SUV_{mean} values of the regions with high [18F]F-FDG avidity and without tracer uptake reflect variable intratumor glycolytic activity and glucose metabolism (SUV_{mean}: 2.72±0.23 and 1.2±0.36 for highly avid and non-avid areas, respectively).

Similarly to our results, in experiments with preclinical models of LS174T (61) and HT29 colorectal tumors (62), MDA-MB-231 breast cancer (62), and A549 (62, 63), H520 and H596 NSCLC (63), Caki renal cell carcinoma (63) or SK-N-BE neuroblastoma (63), increased [18F]F-FDG uptake correlated well with hypoxia.

In agreement with the [18F]F-FDG findings, [18F]F-FAZA examinations also showed differential tracer uptake, that further strengthened the heterogenous distribution of hypoxia within the currently investigated tumors. Although considerable differences were observed between the SUV_{mean} values of the tracer in avid and non-accumulating regions in case of both difluorinated tracers, the distinction was much greater for [18F]F-FAZA, indicating its superior specificity in hypoxia imaging compared to the labelled glucose analogue. The higher specificity of [18F]F-FAZA is

also supported by the fact that it binds to intracellular compounds only under hypoxic conditions, while [^{18}F]F-FDG uptake is increased both in malignant tissues with hypoxia-induced enhanced metabolism, and in benign processes like inflammation or infection.

Of note, considering the non-specificity of [^{18}F]F-FDG accumulation, tumor subvolumes with augmented radioactivity may imply tumor-associated inflammatory processes rather than hypoxia. Moreover, the HIF-1α expression in normoxic cells could also contribute to non-specific [^{18}F]F-FDG accretion (64, 65). Accordingly, available literature findings are contradictory regarding the association between [^{18}F]F-FDG accumulation and hypoxia (65), and some studies questioned the feasibility of the labelled glucose analogue in hypoxia identification (67, 68).

Therefore, based on the above-detailed promising observations on [^{18}F]F-FAZA, we supposed that it could be a suitable complementary of [^{18}F]F-FDG imaging. To assess whether the addition of [^{18}F]F-FAZA to [^{18}F]F-FDG is able to overcome the potential false positive results stemmed from [^{18}F]F-FDG PET acquisition, we compared the images obtained with the two different tracers. In addition, to verify the presence of hypoxia in [^{18}F]F-FDG positive tumor areas we also searched for overlaps between the [^{18}F]F-FAZA and [^{18}F]F-FDG images.

The spatial correlation between [^{18}F]F-FGD and [^{18}F]F-FAZA confirmed the presence of hypoxic areas within the metabolically active tumor regions. Based on our results it appears that although hypoxia is heterogeneously distributed within the investigated tumors, it is most likely to occur in regions with highly active metabolism. Since the strongly [^{18}F]F-FGD positive tumor subregions were more likely to show [^{18}F]F-FAZA uptake, we presume that - because of the fact that the [^{18}F]F-FGD accumulation showed a positive correlation with the presence of hypoxia – the [^{18}F]F-FGD uptake and the related SUV values of a lesion could project whether the increased glucose metabolism is caused by low oxygenation or other non-specific processes.

Additionally, the incomplete overlap between the uptake patterns of the two tracers indicate that tumor hypoxia and glucose metabolism are not always related. Similarly to the present results, discrepancies were detected between [^{18}F]F-FGD and [^{18}F]F-FAZA uptake patterns in aggressive NSCLC in a previous clinical study of Bollineni *et al*. (50). Furthermore, former in-human PET studies on NSCLC also revealed differences between the accumulation of [^{18}F]F-FGD and [^{18}F]F-FMISO, and this was also in accordance with our findings (69, 70).

On the contrary, *Wyss and et al*. found identical distribution patterns for [^{18}F]F-FGD and [^{18}F]F-FMISO in nude mice bearing various xenotransplants of human origin such as KB-31 nasopharyngeal carcinoma, U87 glioblastoma, PC-3 and DU-145 prostate cancer or CLS-2 urinary bladder carcinoma (63). Similarly, the [^{18}F]F-FGD and the [^{18}F]F-FMISO PET images of nude rats inoculated with R3327-AT anaplastic rat prostate tumor or FaDu human squamous cell carcinoma manifested largely comparable uptake profile, however, discrete mismatch could be depicted between them (71).

Although the underlying mechanism of the different accumulation patterns is unclear, the fact that [^{18}F]F-FGD uptake depends on a cluster of factors including microcirculation, HIF-1α expression, transporters and enzymes involved in glucose metabolism, tumor cell/tumor volume ratio or proliferation rate may suggest some explanations (72).

Conclusion

Non-specific findings derived from [^{18}F]F-FGD PET-based tumor diagnostics obviates the need for more precise imaging of tumor-related hypoxia. As [^{18}F]F-FAZA supplies more specific information on tumor hypoxia, supplementing [^{18}F]F-FGD PET imaging with [^{18}F]F-FAZA may have added clinical value in determining hypoxic tumor subregions. The correct identification of low oxygenated tumor areas may not only aid to better understand the biological and pathophysiological processes behind tumor development but also contribute to the prediction of treatment response and clinical outcome. Moreover, such results derived from preclinical studies could be used to monitor therapeutic efficacy or identify those patients who might take advantage of therapeutic strategies such as hypoxia modification and dose-escalated treatments (73).

Conflicts of Interest

The Authors declare no conflicts of interest in relation to this study.

Funding

The research was funded by the Hungarian National Research, Development and Innovation Office (FK-134551 project).

Authors' Contributions

Conceptualization, G.T.; Data curation, I.H.; F.K.; Investigation, J.P.S., É.H.; Methodology, Cs.Cs., V.Sz., T.S., G.O.; Validation, L.B., I.K., J.I.; Visualization, G.T., Z.K.; Writing original draft, Z.K.; Writing review & editing, G.T. All Authors have read and agreed to the published version of the manuscript.

Acknowledgements

Supported by the ÚNKP-23-4-II and ÚNKP-23-5 new national excellence program of the ministry for culture and innovation from the source of the national research, development, and innovation fund.

References

1 Wigerup C, Påhlman S, Bexell D: Therapeutic targeting of hypoxia and hypoxia-inducible factors in cancer. Pharmacol Ther 164: 152-169, 2016. DOI: 10.1016/j.pharmthera.2016.04.009

2 Krock BL, Skuli N, Simon MC: Hypoxia-induced angiogenesis: good and evil. Genes Cancer 2(12): 1117-1133, 2011. DOI: 10.1177/1947601911423654

3 Lamouille S, Xu J, Derynck R: Molecular mechanisms of epithelial-mesenchymal transition. Nat Rev Mol Cell Biol 15(3): 178-196, 2014. DOI: 10.1038/nrm3758

4 Zhang J, Zhang Y, Mo F, Patel G, Butterworth K, Shao C, Prise KM: The roles of HIF-1α in radiosensitivity and radiation-induced bystander effects under hypoxia. Front Cell Dev Biol 9: 637454, 2021. DOI: 10.3389/fcell.2021.637454

5 Taylor PC, Sivakumar B: Hypoxia and angiogenesis in rheumatoid arthritis. Curr Opin Rheumatol 17(3): 293-298, 2005. DOI: 10.1097/01.bor.0000155361.83990.5b

6 Dean M, Hamon Y, Chimini G: The human ATP-binding cassette (ABC) transporter superfamily. J Lipid Res 42(7): 1007-1017, 2001. DOI: 10.1016/S0022-2275(20)31588-1

7 Riou GF, Zhou D, Ahomadegbe JC, Gabillot M, Duvillard P, Lhomme C: Expression of multidrug-resistance (MDR1) gene in normal epithelia and in invasive carcinomas of the uterine cervix. J Natl Cancer Inst 82(18): 1493-1496, 1990. DOI: 10.1093/jnci/82.18.1493

8 Schneider J, Efferth T, Mattern J, Rodriguez-Escudero FJ, Volm M: Immunohistochemical detection of the multi-drug-resistance marker P-glycoprotein in uterine cervical carcinomas and normal cervical tissue. Am J Obstet Gynecol 166(3): 825-829, 1992. DOI: 10.1016/0002-9378(92)91341-7

9 Seborova K, Vaclavikova R, Soucek P, Elsnerova K, Bartakova A, Cernaj P, Bouda J, Rob L, Hruda M, Dvorak P: Association of ABC gene profiles with time to progression and resistance in ovarian cancer revealed by bioinformatics analyses. Cancer Med 8(2): 606-616, 2019. DOI: 10.1002/cam4.1964

10 Emami Nejad A, Najafgholian S, Rostami A, Sistani A, Shojaeifar S, Esparvarinha M, Nedaeinia R, Haghjooy Javanmard S, Taherian M, Ahmadlou M, Salehi R, Sadeghi B, Manian M: The role of hypoxia in the tumor microenvironment and development of cancer stem cell: a novel approach to developing treatment. Cancer Cell Int 21(1): 62, 2021. DOI: 10.1186/s12935-020-01719-5

11 Haubner R, Beer AJ, Wang H, Chen X: Positron emission tomography tracers for imaging angiogenesis. Eur J Nucl Med Mol Imaging 37 Suppl 1(0 1): S86-103, 2010. DOI: 10.1007/s00259-010-1503-4

12 Alauddin MM: Positron emission tomography (PET) imaging with (18)F-based radiotracers. Am J Nucl Med Mol Imaging 2(1): 55-76, 2012.

13 Conti M, Eriksson L: Physics of pure and non-pure positron emitters for PET: a review and a discussion. EJNMMI Phys 3(1): 8, 2016. DOI: 10.1186/s40658-016-0144-5

14 Jacobson O, Kiesewetter DO, Chen X: Fluorine-18 radiochemistry, labeling strategies and synthetic routes. Bioconjug Chem 26(1): 1-18, 2015. DOI: 10.1021/bc500475e

15 Richter S, Wuest F: 18F-labeled peptides: the future is bright. Molecules 19(12): 20536-20556, 2014. DOI: 10.3390/molecules191220536

16 Ruan K, Song G, Ouyang G: Role of hypoxia in the hallmarks of human cancer. J Cell Biochem 107(6): 1053-1062, 2009. DOI: 10.1002/jcb.22214

17 Semenza GL: Defining the role of hypoxia-inducible factor 1 in cancer biology and therapeutics. Oncogene 29(5): 625-634, 2010. DOI: 10.1038/onc.2009.441

18 Burgman P, Odonoghue JA, Humm JL, Ling CC: Hypoxia-induced increase in FDG uptake in MCF7 cells. J Nucl Med 42(1): 170-175, 2001.

19 Murakami T, Nishiyama T, Shirotani T, Shinohara Y, Kan M, Ishii K, Kanai F, Nakazuru S, Ebina Y: Identification of two enhancer elements in the gene encoding the type 1 glucose transporter from the mouse which are responsive to serum, growth factor, and oncogenes. J Biol Chem 267(13): 9300-9306, 1992.

20 Mellanen P, Minn H, Grénman R, Härkönen P: Expression of glucose transporters in head-and-neck tumors. Int J Cancer 56(5): 622-629, 1994. DOI: 10.1002/ijc.2910560503

21 Clavo AC, Brown RS, Wahl RL: Fluorodeoxyglucose uptake in human cancer cell lines is increased by hypoxia. J Nucl Med 36(9): 1625-1632, 1995.

22 Brown RS, Fisher SJ, Wahl RL: Autoradiographic evaluation of the intra-tumoral distribution of 2-deoxy-D-glucose and monoclonal antibodies in xenografts of human ovarian adenocarcinoma. J Nucl Med 34(1): 75-82, 1993.

23 Clavo AC, Wahl RL: Effects of hypoxia on the uptake of tritiated thymidine, L-leucine, L-methionine and FDG in cultured cancer cells. J Nucl Med 37(3): 502-506, 1996.

24 Kubota R, Kubota K, Yamada S, Tada M, Ido T, Tamahashi N: Active and passive mechanisms of [fluorine-18] fluorodeoxyglucose uptake by proliferating and prenecrotic cancer cells *in vivo*: a microautoradiographic study. J Nucl Med 35(6): 1067-1075, 1994.

25 Pijl JP, Nienhuis PH, Kwee TC, Glaudemans AWJM, Slart RHJA, Gormsen LC: Limitations and pitfalls of FDG-PET/CT in infection and inflammation. Semin Nucl Med 51(6): 633-645, 2021. DOI: 10.1053/j.semnuclmed.2021.06.008

26 Kumar P, Stypinski, D, Xia H, McEwan AJB, Machulla HJ, Wiebe LI: Fluoroazomycin arabinoside (FAZA): synthesis, 2H and 3H-labelling and preliminary biological evaluation of a novel 2-nitroimidazole marker of tissue hypoxia. J Label Compd Radiopharm 42(1): 3-16, 1999. DOI: 10.1002/(SICI)1099-1344(199901)42:1<3::AID-JLCR160>3.0.CO;2-H

27 Foo SS, Abbott DF, Lawrentschuk N, Scott AM: Functional imaging of intratumoral hypoxia. Mol Imaging Biol 6(5): 291-305, 2004. DOI: 10.1016/j.mibio.2004.06.007

28 Whitmore GF, Varghese AJ: The biological properties of reduced nitroheterocyclics and possible underlying biochemical mechanisms. Biochem Pharmacol 35(1): 97-103, 1986. DOI: 10.1016/0006-2952(86)90565-4

29 Huang Y, Fan J, Li Y, Fu S, Chen Y, Wu J: Imaging of tumor hypoxia with radionuclide-labeled tracers for PET. Front Oncol 11: 731503, 2021. DOI: 10.3389/fonc.2021.731503

30 Souvatzoglou M, Grosu AL, Röper B, Krause BJ, Beck R, Reischl G, Picchio M, Machulla HJ, Wester HJ, Piert M: Tumour hypoxia imaging with [18F]FAZA PET in head and neck cancer patients: a pilot study. Eur J Nucl Med Mol Imaging 34(10): 1566-1575, 2007. DOI: 10.1007/s00259-007-0424-3

31 Dos Santos SN, Wuest M, Jans H, Woodfield J, Nario AP, Krys D, Dufour J, Glubrecht D, Bergman C, Bernardes ES, Wuest F:

Comparison of three 18F-labeled 2-nitroimidazoles for imaging hypoxia in breast cancer xenografts: [18F]FBNA, [18F]FAZA and [18F]FMISO. Nucl Med Biol 124-125: 108383, 2023. DOI: 10.1016/j.nucmedbio.2023.108383

32 Busk M, Mortensen LS, Nordsmark M, Overgaard J, Jakobsen S, Hansen KV, Theil J, Kallehauge JF, D'Andrea FP, Steiniche T, Horsman MR: PET hypoxia imaging with FAZA: reproducibility at baseline and during fractionated radiotherapy in tumour-bearing mice. Eur J Nucl Med Mol Imaging 40(2): 186-197, 2013. DOI: 10.1007/s00259-012-2258-x

33 Solomon B, Binns D, Roselt P, Weibe LI, McArthur GA, Cullinane C, Hicks RJ: Modulation of intratumoral hypoxia by the epidermal growth factor receptor inhibitor gefitinib detected using small animal PET imaging. Mol Cancer Ther 4(9): 1417-1422, 2005. DOI: 10.1158/1535-7163.MCT-05-0066

34 Melsens E, De Vlieghere E, Descamps B, Vanhove C, Kersemans K, De Vos F, Goethals I, Brans B, De Wever O, Ceelen W, Pattyn P: Hypoxia imaging with (18)F-FAZA PET/CT predicts radiotherapy response in esophageal adenocarcinoma xenografts. Radiat Oncol 13(1): 39, 2018. DOI: 10.1186/s13014-018-0984-3

35 Sorger D, Patt M, Kumar P, Wiebe LI, Barthel H, Seese A, Dannenberg C, Tannapfel A, Kluge R, Sabri O: [18F]Fluoroazomycinarabinofuranoside (18FAZA) and [18F]Fluoromisonidazole (18FMISO): a comparative study of their selective uptake in hypoxic cells and PET imaging in experimental rat tumors. Nucl Med Biol 30(3): 317-326, 2003. DOI: 10.1016/s0969-8051(02)00442-0

36 Hamacher K, Coenen HH, Stöcklin G: Efficient stereospecific synthesis of no-carrier-added 2-[18F]-fluoro-2-deoxy-D-glucose using aminopolyether supported nucleophilic substitution. J Nucl Med 27(2): 235-238, 1986.

37 Reischl G, Ehrlichmann W, Bieg C, Solbach C, Kumar P, Wiebe LI, Machulla HJ: Preparation of the hypoxia imaging PET tracer [18F]FAZA: reaction parameters and automation. Appl Radiat Isot 62(6): 897-901, 2005. DOI: 10.1016/j.apradiso.2004.12.004

38 Huang Y, Du KM, Xue ZH, Yan H, Li D, Liu W, Chen Z, Zhao Q, Tong JH, Zhu YS, Chen GQ: Cobalt chloride and low oxygen tension trigger differentiation of acute myeloid leukemic cells: possible mediation of hypoxia-inducible factor-1α. Leukemia 17(11): 2065-2073, 2003. DOI: 10.1038/sj.leu.2403141

39 Zhang YB, Wang X, Meister EA, Gong KR, Yan SC, Lu GW, Ji XM, Shao G: The effects of CoCl2 on HIF-1α protein under experimental conditions of autoprogressive hypoxia using mouse models. Int J Mol Sci 15(6): 10999-11012, 2014. DOI: 10.3390/ijms150610999

40 UKCCCR guidelines for the welfare of animals in experimental neoplasia. Br J Cancer 58(1): 109-113, 1988. DOI: 10.1038/bjc.1988.174

41 Guo M, Song LP, Jiang Y, Liu W, Yu Y, Chen GQ: Hypoxia-mimetic agents desferrioxamine and cobalt chloride induce leukemic cell apoptosis through different hypoxia-inducible factor-1α independent mechanisms. Apoptosis 11(1): 67-77, 2006. DOI: 10.1007/s10495-005-3085-3

42 Vengellur A, LaPres JJ: The role of hypoxia inducible factor 1alpha in cobalt chloride induced cell death in mouse embryonic fibroblasts. Toxicol Sci 82(2): 638-646, 2004. DOI: 10.1093/toxsci/kfh278

43 Busch W, Kühnel D, Schirmer K, Scholz S: Tungsten carbide cobalt nanoparticles exert hypoxia-like effects on the gene expression level in human keratinocytes. BMC Genomics 11: 65, 2010. DOI: 10.1186/1471-2164-11-65

44 Hayashi M, Sakata M, Takeda T, Yamamoto T, Okamoto Y, Sawada K, Kimura A, Minekawa R, Tahara M, Tasaka K, Murata Y: Induction of glucose transporter 1 expression through hypoxia-inducible factor 1α under hypoxic conditions in trophoblast-derived cells. J Endocrinol 183(1): 145-154, 2004. DOI: 10.1677/joe.1.05599

45 Mathupala SP, Rempel A, Pedersen PL: Glucose catabolism in cancer cells. J Biol Chem 276(46): 43407-43412, 2001. DOI: 10.1074/jbc.M108181200

46 Minn H, Clavo AC, Wahl RL: Influence of hypoxia on tracer accumulation in squamous-cell carcinoma: *in vitro* evaluation for PET imaging. Nucl Med Biol 23(8): 941-946, 1996. DOI: 10.1016/s0969-8051(96)00134-5

47 Hara T, Bansal A, DeGrado TR: Effect of hypoxia on the uptake of [methyl-3H]choline, [1-14C] acetate and [18F]FDG in cultured prostate cancer cells. Nucl Med Biol 33(8): 977-984, 2006. DOI: 10.1016/j.nucmedbio.2006.08.002

48 Pedersen MW, Holm S, Lund EL, Højgaard L, Kristjansen PE: Coregulation of glucose uptake and vascular endothelial growth factor (VEGF) in two small-cell lung cancer (SCLC) sublines *in vivo* and *in vitro*. Neoplasia 3(1): 80-87, 2001. DOI: 10.1038/sj.neo.7900133

49 Hammond EM, Asselin MC, Forster D, O'Connor JP, Senra JM, Williams KJ: The meaning, measurement and modification of hypoxia in the laboratory and the clinic. Clin Oncol (R Coll Radiol) 26(5): 277-288, 2014. DOI: 10.1016/j.clon.2014.02.002

50 Bollineni VR, Kerner GS, Pruim J, Steenbakkers RJ, Wiegman EM, Koole MJ, De Groot EH, Willemsen AT, Luurtsema G, Widder J, Groen HJ, Langendijk JA: PET imaging of tumor hypoxia using ^{18}F-fluoroazomycin arabinoside in stage III-IV non-small cell lung cancer patients. J Nucl Med 54(8): 1175-1180, 2013. DOI: 10.2967/jnumed.112.115014

51 Kerner GS, Bollineni VR, Hiltermann TJ, Sijtsema NM, Fischer A, Bongaerts AH, Pruim J, Groen HJ: An exploratory study of volumetric analysis for assessing tumor response with (18)F-FAZA PET/CT in patients with advanced non-small-cell lung cancer (NSCLC). EJNMMI Res 6(1): 33, 2016. DOI: 10.1186/s13550-016-0187-6

52 Lee N, Nehmeh S, Schöder H, Fury M, Chan K, Ling CC, Humm J: Prospective trial incorporating pre-/mid-treatment [18F]-misonidazole positron emission tomography for head-and-neck cancer patients undergoing concurrent chemoradiotherapy. Int J Radiat Oncol Biol Phys 75(1): 101-108, 2009. DOI: 10.1016/j.ijrobp.2008.10.049

53 Busk M, Horsman MR, Jakobsen S, Hansen KV, Bussink J, van der Kogel A, Overgaard J: Can hypoxia-PET map hypoxic cell density heterogeneity accurately in an animal tumor model at a clinically obtainable image contrast? Radiother Oncol 92(3): 429-436, 2009. DOI: 10.1016/j.radonc.2009.08.026

54 Piert M, Machulla HJ, Picchio M, Reischl G, Ziegler S, Kumar P, Wester HJ, Beck R, McEwan AJ, Wiebe LI, Schwaiger M: Hypoxia-specific tumor imaging with 18F-fluoroazomycin arabinoside. J Nucl Med 46(1): 106-113, 2005.

55 Reischl G, Dorow DS, Cullinane C, Katsifis A, Roselt P, Binns D, Hicks RJ: Imaging of tumor hypoxia with [124I]IAZA in comparison with [18F]FMISO and [18F]FAZA—first small animal PET results. J Pharm Pharm Sci 10(2): 203-211, 2007.

56 Peeters SG, Zegers CM, Lieuwes NG, van Elmpt W, Eriksson J, van Dongen GA, Dubois L, Lambin P: A comparative study of the hypoxia PET tracers [18F]HX4, [18F]FAZA, and [18F]FMISO in a preclinical tumor model. Int J Radiat Oncol Biol Phys 91(2): 351-359, 2015. DOI: 10.1016/j.ijrobp.2014.09.045

57 Servagi-Vernat S, Differding S, Hanin FX, Labar D, Bol A, Lee JA, Grégoire V: A prospective clinical study of 18 F-FAZA PET-CT hypoxia imaging in head and neck squamous cell carcinoma before and during radiation therapy. Eur J Nucl Med Mol Imaging 41(8): 1544-1552, 2014. DOI: 10.1007/s00259-014-2730-x

58 Trinkaus ME, Blum R, Rischin D, Callahan J, Bressel M, Segard T, Roselt P, Eu P, Binns D, MacManus MP, Ball D, Hicks RJ: Imaging of hypoxia with ^{18}F-FAZA PET in patients with locally advanced non-small cell lung cancer treated with definitive chemoradiotherapy. J Med Imaging Radiat Oncol 57(4): 475-481, 2013. DOI: 10.1111/1754-9485.12086

59 Choen S, Kent MS, Chaudhari AJ, Cherry SR, Krtolica A, Zwingenberger AL: Kinetic evaluation of the hypoxia radiotracers [(18)F]FMISO and [(18)F]FAZA in dogs with spontaneous tumors using dynamic PET/CT imaging. Nucl Med Mol Imaging 57(1): 16-25, 2023. DOI: 10.1007/s13139-022-00780-4

60 Semenza GL: Hypoxia, clonal selection, and the role of HIF-1 in tumor progression. Crit Rev Biochem Mol Biol 35(2): 71-103, 2000. DOI: 10.1080/10409230091169186

61 Dearling JL, Flynn AA, Sutcliffe-Goulden J, Petrie IA, Boden R, Green AJ, Boxer GM, Begent RH, Pedley RB: Analysis of the regional uptake of radiolabeled deoxyglucose analogs in human tumor xenografts. J Nucl Med 45(1): 101-107, 2004.

62 Li XF, Du Y, Ma Y, Postel GC, Civelek AC: (18)F-fluorodeoxyglucose uptake and tumor hypoxia: revisit (18)f-fluorodeoxyglucose in oncology application. Transl Oncol 7(2): 240-247, 2014. DOI: 10.1016/j.tranon.2014.02.010

63 Wyss MT, Honer M, Schubiger PA, Ametamey SM: NanoPET imaging of [18F]fluoromisonidazole uptake in experimental mouse tumours. Eur J Nucl Med Mol Imaging 33(3): 311-318, 2006. DOI: 10.1007/s00259-005-1951-4

64 Brown JM, Wilson WR: Exploiting tumour hypoxia in cancer treatment. Nat Rev Cancer 4(6): 437-447, 2004. DOI: 10.1038/nrc1367

65 Talks KL, Turley H, Gatter KC, Maxwell PH, Pugh CW, Ratcliffe PJ, Harris AL: The expression and distribution of the hypoxia-inducible factors HIF-1alpha and HIF-2alpha in normal human tissues, cancers, and tumor-associated macrophages. Am J Pathol 157(2): 411-421, 2000. DOI: 10.1016/s0002-9440(10)64554-3

66 Mees G, Dierckx R, Vangestel C, van de Wiele C: Molecular imaging of hypoxia with radiolabelled agents. Eur J Nucl Med Mol Imaging 36(10): 1674-1686, 2009. DOI: 10.1007/s00259-009-1195-9

67 Lopci E, Grassi I, Chiti A, Nanni C, Cicoria G, Toschi L, Fonti C, Lodi F, Mattioli S, Fanti S: PET radiopharmaceuticals for imaging of tumor hypoxia: a review of the evidence. Am J Nucl Med Mol Imaging 4(4): 365-384, 2014.

68 Christian N, Deheneffe S, Bol A, De Bast M, Labar D, Lee JA, Grégoire V: Is (18)F-FDG a surrogate tracer to measure tumor hypoxia? Comparison with the hypoxic tracer (14)C-EF3 in animal tumor models. Radiother Oncol 97(2): 183-188, 2010. DOI: 10.1016/j.radonc.2010.02.020

69 Gagel B, Reinartz P, Demirel C, Kaiser HJ, Zimny M, Piroth M, Pinkawa M, Stanzel S, Asadpour B, Hamacher K, Coenen HH, Buell U, Eble MJ: [18F] fluoromisonidazole and [18F] fluorodeoxyglucose positron emission tomography in response evaluation after chemo-/radiotherapy of non-small-cell lung cancer: a feasibility study. BMC Cancer 6: 51, 2006. DOI: 10.1186/1471-2407-6-51

70 Cherk MH, Foo SS, Poon AM, Knight SR, Murone C, Papenfuss AT, Sachinidis JI, Saunder TH, O'Keefe GJ, Scott AM: Lack of correlation of hypoxic cell fraction and angiogenesis with glucose metabolic rate in non-small cell lung cancer assessed by 18F-Fluoromisonidazole and 18F-FDG PET. J Nucl Med 47(12): 1921-1926, 2006.

71 Zanzonico P, Campa J, Polycarpe-Holman D, Forster G, Finn R, Larson S, Humm J, Ling C: Animal-specific positioning molds for registration of repeat imaging studies: comparative microPET imaging of F18-labeled fluoro-deoxyglucose and fluoro-misonidazole in rodent tumors. Nucl Med Biol 33(1): 65-70, 2006. DOI: 10.1016/j.nucmedbio.2005.07.011

72 Bos R, van der Hoeven JJ, van der Wall E, van der Groep P, van Diest PJ, Comans EF, Joshi U, Semenza GL, Hoekstra OS, Lammertsma AA, Molthoff CF: Biologic correlates of ^{18}Fluorodeoxyglucose uptake in human breast cancer measured by positron emission tomography. J Clin Oncol 20(2): 379-387, 2002. DOI: 10.1200/JCO.2002.20.2.379

73 Zips D, Zöphel K, Abolmaali N, Perrin R, Abramyuk A, Haase R, Appold S, Steinbach J, Kotzerke J, Baumann M: Exploratory prospective trial of hypoxia-specific PET imaging during radiochemotherapy in patients with locally advanced head-and-neck cancer. Radiother Oncol 105(1): 21-28, 2012. DOI: 10.1016/j.radonc.2012.08.019

Received November 6, 2023
Revised December 10, 2023
Accepted December 11, 2023